Functional Materials Letters
Vol. 10, No. 1, (2016) 1650053 (5 pages)

DOI: 10.1142/S1793604716500533

World Scientific
www.worldscientific.com

Excess lithium storage in $LiFePO_4$-Carbon interface by ball-milling

Hua Guo, Xiaohe Song, Jiaxin Zheng and Feng Pan*
School of Advanced Materials
Peking University Shenzhen Graduate School, Shenzhen 518055, P. R. China
**panfeng@pkusz.edu.cn*

Received 5 May 2016; Accepted 28 May 2016; Published

As one of the most popular cathode materials for high power lithium ion batteries (LIBs) of the electrical-vehicle (EV), lithium iron phosphate ($LiFePO_4$ (LFP)) is limited to its relatively lower theoretical specific capacity of 170 mAh g^{-1}. To break the limits and further improve the capacity of LFP is promising but challenging. In this study, the ball-milling method is applied to the mixture of LFP and carbon, and the effective capacity larger than the theoretical one by 30 mAh g^{-1} is achieved. It is demonstrated that ball-milling leads to the LFP-Carbon interface to store the excess Li-ions.

Keywords: Lithium iron phosphate; ball-milling; interface; excess capacity.

Olive lithium iron phosphate (named as $LiFePO_4$, abbreviated as LFP) is one of the most popular cathode materials for high power lithium ion batteries (LIBs) of the electrical-vehicle (EV), with the advantage that it is environment friendly, low-cost, and safe.[1–3] A lot of efforts such as carbon coating,[4] nanocrystallization,[5] defects elimination,[6] and so on, have been paid to improve the electrochemical performance of LFP since the first work of Padhi *et al.*[7] Although cathodes on the basis of LFP had achieved specific capacity close to the theoretical value of 170 mAh g^{-1}, it is still relatively low compared to the other popular cathode materials,[8] such as $LiNi_xMn_yCo_zO_2$.[9] Because the LFP has a highly stable[10] olive structure where the P–O bond of phosphate [PO_4] is strong,[11] the lithiation/delithiation is achieved only through the valence change of Fe ion between bivalence (Fe^{2+}) and trivalence (Fe^{3+}), further improvement of the intrinsic capacity of LFP is limited to the theoretical specific capacity.

The final capacity is an overall effect of the LFP-based cathode electrode which is made of LFP particle, carbon black, and binder. Although the intrinsic capacity of LFP is limited, it would be a potential method to improve the capacity of the total electrode if we could make use of the nano-interface between the LFP and the carbon black by creating additional active Li-ion storage sites.[12] Ball-milling technique[13] is a mechanochemical method to modify the particle surface[14] and could be used to create new interface between cathode material and carbon black. In our previous work,[15] we made new beta-LFP activated to create new diffusion paths and storage sites of Li-ions by ball-milling the nanoparticles with conductive carbon. In this work, ball-milling treatment is applied to the mixture of LFP and acetylene black, and a capacity as high as 200 mAh g^{-1} is achieved.

LFP was synthesized via solvothermal method.[16] Ferrous sulfate, lithium hydroxide and phosphate acid was dissolved in ethanol glycol separately. A dark green slurry was formed by mixing the solutions. After 2 h stirring, to make sure of thorough mixing and heating to 180°C for 8 h, product can be collected from centrifugation, washed with water and ethanol and dried at 80°C in vacuum oven overnight. Morphologies of LFP nanocrystals are tested by scanning electron microscopy (SEM) as shown in Fig. 1(b). Synthesized nanocrystals are in shape of nanoparticles with edges and corners, with size of about 80 nm. The X-ray diffraction (XRD) was carried out on Bruker D8 Advance with Cu-Kα radiation, and the result shows that the as-prepared LFP particle are in Pmnb space group (PDF#83-1173). As shown in Fig. S1, it is pure and no other secondary phase exists. High resolution transmission electron microscopy (HRTEM, inset of Fig. 1(b)), carried out by FEI Tecnai G2 F30, shows some crystallographic planes of the LFP crystal, and proves particles are monocrystal and well crystallized.

The electrochemical tests of the materials were carried out on the coin cells. The samples were dispersed in polyvinylidene fluoride solution. The formed slurry was coated on aluminum foil as cathode and was dried in vacuum oven. The coating weight of the electrode is 1 mg cm^{-2}. Lithium metal was used as anode and $LiPF_6$ solution as electrolyte to

*Corresponding author.

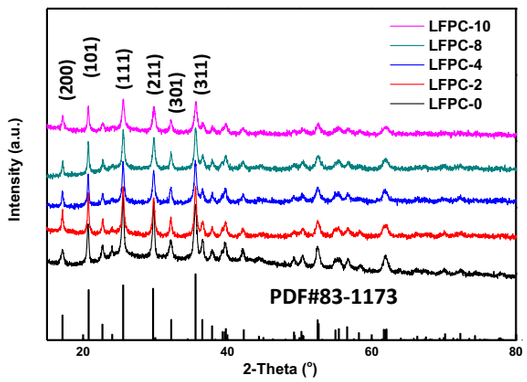

(a)

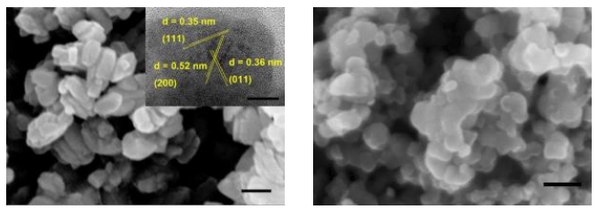

(b) (c)

Fig. 1. (a) XRD change of the complex materials during milling process. (b) Morphology of materials before and (c) after milling detected by SEM.

assemble the coin cells. It is worth noting that all of the as-prepared particles in this study are not carbon-coated. To compare with the following section, it is physically blended with carbon black (acetylene black, nanospheres in size of 80 nm) in weight ratio of 100:70. Although such high carbon loadings are inappropriate for real batteries, they are useful in establishing the true rate capability of the active material and are commonly used in the testing of high-rate nanomaterials.[17] Galvanostatic charging/discharging tests in voltage ranges of 2.0–4.2 V were applied to test the electrochemical performance. The electrochemical performance of pure carbon black was also tested, exhibiting a tiny capacity of about 5 mAh g^{-1} at 17 mA g^{-1}, as shown in Fig. S2. To calculate the effective specific capacity of the as-prepared LFP (LFPC-0), corresponding capacity of carbon black was excluded. It is revealed that the LFPC-0 possesses a capacity of about 135 mAh g^{-1}, with the typical voltage platform at 3.45 V, as shown in Figs. 2(a) and 2(b).

The product LFP was mixed completely with carbon black in weight ratio of 100:70, and transferred into zirconia vessel for planetary ball-milling at 350 rpm. After ball-milling, LFP and carbon black were mixed thoroughly, and the sample ball-milled for *n* hours is named LFPC-*n*. As shown in Fig. 1(c), the particles aggregated and initially clear edges of the particles blurred. It is believed that carbon black is tightly contacted with the LFP particles after ball-milling.

Figure 1(a) shows XRD results of samples with different milling time. It shows that all peaks of LFP remain almost the same positions, in great agreement with standard peak positions from PDF#83-1173. So the structure of LFP does not change during the milling process. Intensity of peaks decreases as milling time increases, which illustrates the degree of crystallinity decreases in the process, which is a common phenomenon in ball-milling treatment.[14] As discussed in the following, the defected domains are formed during the ball-milling.

The same ball-milling process as the cathode sample is also applied to carbon black. Figure 2(b) shows that in the voltage range between 2.0 V and 4.2 V, the milled carbon has a capacity of 27 mAh g^{-1} at the current of 17 mA g^{-1}. With the corresponding capacity of ball-milled carbon excluded, the samples with the ball-milling time of 2, 4, 8, and 10 h have the capacity of 146, 149, 170, and 200 mAh g^{-1}, respectively. The capacity was calculated on the basis of LFP and the capacity corresponding to carbon black has been excluded (calculation method for the effective capacity of the ball-milled LFPC-*n* is discussed in detail in the Supporting Information). It means that the effective capacity increases as milling time increases.

The charging/discharging curves of the milled samples LFPC-*n* have partial platform with a big slope, which are different from that of LFPC-0 (Figs. 2(a) and 2(b)). Different current are applied to LFPC-10 to test the rate and cycling performance, and it shows great cycling performance with no capacity fading after 1000 cycle at 1 C (170 mA g^{-1}) as shown in Figs. 2(c) and 2(d). The capacity of the platform part at 3.45 V remains about 70 mAh g^{-1} and almost does not change as the ball-milling time increases from 2 h to 10 h (Figs. 2(a) and 2(b)). The platform in the charging/discharging curves illustrates that the amount of pure LFP crystal decreased initially in the ball-milling process and remain constant after about 2 h, which means that the initial ball-milling destroys the crystal structure on the outer layer of LFP nanocrystals, and then it reaches equilibrium subsequently. The capacity of the slope part increases as the ball-milling time increases. The slope is partly contributed by the non-oliven phase caused by ball-milling. The non-oliven phase, such as the amorphous LFP, has a high initial capacity close to 170 mAh g^{-1}, but the amorphous often has a relatively bad cycling performance.[18] However, the milled samples shows good cycling performance as discussed above, therefore the defective phase may be some special defective phase other than the amorphous one.

Interestingly, LFPC-10 achieved a capacity of 200 mAh g^{-1}, which is larger than LFP theoretical capacity of 170 mAh g^{-1}, meaning that excess Li-ion storage sites are created by ball-milling. Because the capacity of carbon has been excluded, it is speculated that the excess Li-ion storage

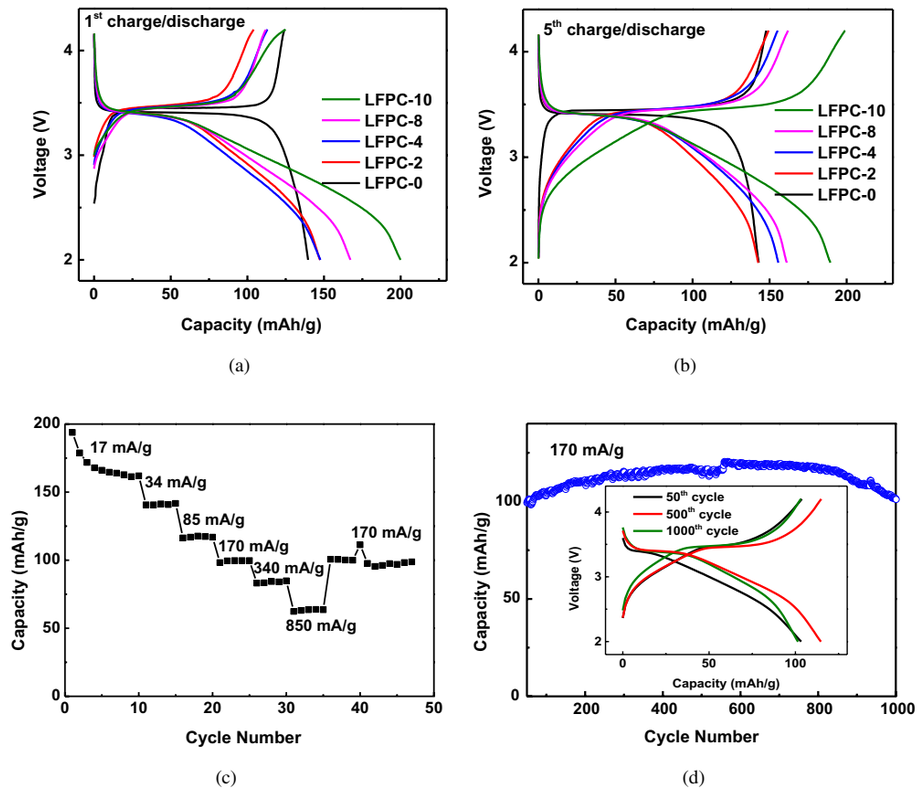

Fig. 2. Electrochemical test of samples LFPC-*n*, *n* denotes the different ball-milling time. Voltage-capacity curve of (a) first cycle and (b) 5th cycle. (c) Rate performance of LFPC-10 at different current. (d) Cycling performance of LFPC-10 at the current of 170 mA g^{-1}.

sites lie in the LFP-Carbon interface. To better explain excess Li-ion storage sites in the surface, X-ray photoelectron spectronscopy (XPS) is applied to investigate the surface of LFP and carbon black.

XPS test demonstrates that, for LFPC-0, Fe-ions in both the surface and the bulk are bivalence (Fe^{2+}), which is reasonable for lithiated state (Figs. 3(a) and S3(a)). But for the ball-milled LFPC-10, Fe ions in the bulk remains bivalence (Fig. S3(a)), but Fe ions on the surface of the LFPC-10 transforms to trivalence (Fe^{3+}). As shown in Fig. 3(a), the peaks of Fe 2p XPS spectra shifted from 710 eV and 724 eV to higher value 712 eV and 726 eV, respectively.[19] Therefore, Li-ions are extracted from the LFP surface during the ball-milling process. The extraction of Li-ions from the surface is

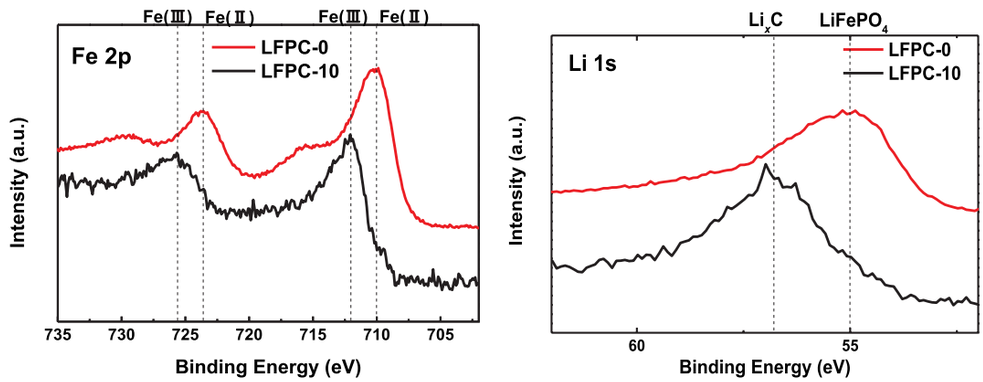

Fig. 3. Comparison of XPS spectra between non-milled LFPC-0 and milled LFPC-10. (a), (b), (c), and (d) shows the spectra of Fe 2p, Li 1s, O 1s, and C 1s, respectively.

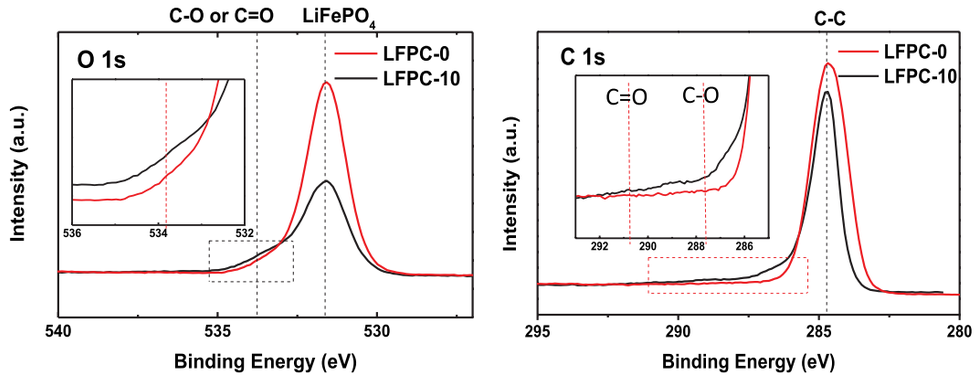

(c) (d)

Fig. 3. (*Continued*)

further proved by Li 1s XPS spectra (Figs. 3(b) and S3(b)), where the peak at 57 eV attributed to Li_xC is detected on the surface. While for the non-milled bLFPC-0, no Li_xC is detected. This result demonstrates that lithium transfers from LFP to carbon black surface, forming Li–C bond in the ball-milled process. The strong interaction between LFP and carbon black is in agreement with serious aggregation of the particles detected by SEM (Fig. 1(c)).

In addition, it is found that the first charging process of different ball-milled samples exhibit almost the same capacity, although the discharging capacity increases along with the ball-milling time (Fig. 2(a)). It is illustrated that Li-ion extracted from LFP to LFP-Carbon interface is still active and could contribute to the capacity. Smaller nanoparticles, large specific surface area, and more lithium storage sites are provided on the surface.[20]

Besides, Figs. 3(c) and 3(d) illustrate the O 1s XPS spectra. For the LFPC-0, the O 1s peak is only contributed by LFP. As shown in Fig. 3(c), it is interesting that the O 1s peak of the ball-milled LFPC-10 is asymmetric and a new peak at 533 eV can be detected. The peak is attributed to the C–O or C=O bond, which illustrates the chemical interaction between the carbon and oxygen. On the other hand, the C 1s XPS spectra shows an additional peak around 288 eV, which is also attributed to the C–O and C=O bond, in the ball-milled sample LFPC-10. Therefore, both the O 1s and C 1s XPS spectra demonstrate the presence of C–O or C=O bond after ball-milling. Lung-Hao Hu *et al.* has reported[21] that C–O (C=O) bond can provide lithium storage with formation of lithium–oxygen bond, and the reaction voltage was proved to be around 3 V, which is in agreement with electrochemical performance of LFPC-10 in this study.

Given all the results above, it is believed that the ball-milling leads the initially separated LFP and carbon black particles to close contacting with each other, and the chemical interaction between particles creates the LFP-Carbon interface as excess Li-ion storage sites (Fig. 4). It is these Li-ion storage sites that contribute to the excess capacity beyond the theoretical one.

In summary, the ball-milling method is applied to LFP nanocrystals mixed with carbon black. Interestingly, the milled nanocrystals achieved a specific capacity larger than the theoretical value by 30 mAh g^{-1}. The SEM image illustrated that the initially separated LFP and carbon black aggregated after ball-milling, leading to the close contact between the LFP and carbon black nanoparticles. The XPS spectra demonstrated that Li-ions on the LFP surface transformed into the carbon, and the newly formed C–O bonds are detected, which illustrate the chemical interaction between the LFP and carbon black. Therefore, the new LFP-Carbon interface is created. The excess Li-ion storage sites lies in the LFP-Carbon interface and therefore leads to excess capacity beyond the theoretical value.

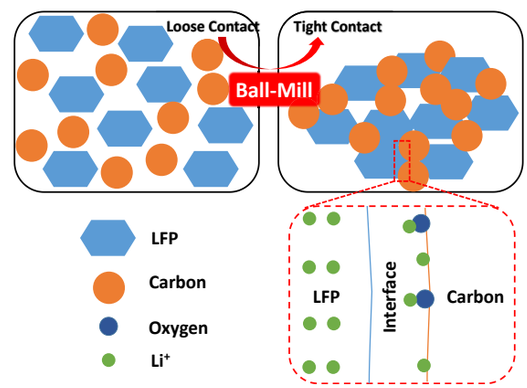

Fig. 4. Schematic of the process that, after ball-milling, the initial mixture of separated LFP nanocrystals and carbon black transferred into tightly aggregated state with chemical interaction between each other, forming the LFP-Carbon interface wherein lies the active Li-ion sites.

Acknowledgment

The research was financially supported by Guangdong Innovation Team Project (No. 202013N080), and Shenzhen Science and Technology Research Grant (No. ZDSY20130331145131323).

References

1. C. Masquelier *et al.*, *Chem. Rev.* **113**, 6552 (2013).
2. Y. Wang *et al.*, *Energy Environ. Sci.* **4**, 805 (2011).
3. J. M. Tarascon *et al.*, *Nature* **414**, 359 (2001).
4. J. Wang *et al.*, *Energy Environ. Sci.* **5**, 5163 (2012).
5. Y. S. Yu *et al.*, *Nano Lett.* **15**, 4282 (2015).
6. K.-Y. Park *et al.*, *Chem. Mater.* **26**, 5345 (2014).
7. A. K. Padhi *et al.*, *J. Electrochem. Soc.* **144**, 1188 (1997).
8. J. B. Goodenough *et al.*, *J. Am. Chem. Soc.* **135**, 1167 (2013).
9. X. Li *et al.*, *Funct. Mater. Lett.* **7**, 1440013 (2014).
10. J. R. Owen, *Chem. Soc. Rev.* **26**, 259 (1997).
11. S. Y. Chung *et al.*, *J. Am. Chem. Soc.* **135**, 7811 (2013).
12. S. Muroi *et al.*, *Electrochemistry* **83**, 609 (2015).
13. C. Suryanarayana, *Prog. Mater. Sci.* **46**, 1 (2001).
14. J. Ni *et al.*, *J. Power Sources* **196**, 8104 (2011).
15. H. Guo *et al.*, *Nano Lett.* **16**, 601 (2016).
16. L. Wang *et al.*, *Nano Lett.* **12**, 5632 (2012).
17. B. Kang *et al.*, *Nature* **458**, 190 (2009).
18. V. Mathew *et al.*, *NPG Asia Mater.* **6**, e138 (2014).
19. R. Dedryvere *et al.*, *Chem. Mater.* **20**, 7164 (2008).
20. Z. N. Yu *et al.*, *Energy Environ. Sci.* **8**, 702 (2015).
21. B. Lung-Hao Hu *et al.*, *Nat Commun.* **4**, 1687 (2013).